Three-dimensional modeling study of the effect of irradiation on a single-face polycrystalline silicon photocell under multispectral illumination

ABSTRACT

A three-dimensional modeling study of a polycrystalline silicon mono-facet photocell under multi-spectral illumination is presented highlighting the effect of irradiation energy (Φ) and damage coefficient (Kl) on the macroscopic parameters of the photocell. From this three-dimensional model, the expression of the excess minority charge carrier density in the base of the polycrystalline silicon single-face photocell is obtained. From the latter we determined the current density and the photovoltage. This study takes into account the irradiation energy and the damage coefficient on the quality of the polycrystalline silicon photocell.

Keywords: Grain Size, Grain Boundary Recombination Velocity, Polycrystalline, Solar Cell, Irradiation, Current Density, Photovoltage.

1. INTRODUCTION

Several technics of characterization of the silicon material, determination of the phenomenological and electrical parameters have been used to improve the capacity of solar cells.

Some of these techniques have been developed in static regime [1], and others in dynamic frequency regime [2]. Extensive studies on the capacity of the space charge area [3-4] and recombination parameters [5] [6] have been performed in 3 dimensions [1-6-7-8-10] for these two regimes. Our contribution consists in determining the current density and photovoltage of a silicon photocell in static regime placed under (Kl, Φ) irradiation and multi-spectral illumination.

We briefly present a theoretical study in which we schematize a grain of the photocell and solve the diffusion equation. Then we discuss the obtained results before concluding.

2. THEORITICAL ANALYSIS

The BSF polycrystalline silicon solar cell studied is an n^+-p-p^+ structure as shown in Figure 1.a. Silicon consisting of several grain of various sizes, for our study, we use the 3D columnar model where each grain has a rectangular shape as shown in figure1.b below [6] [11] [12].

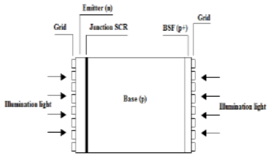 Figure 1.a. Bifacial Silicon solar cell Structure	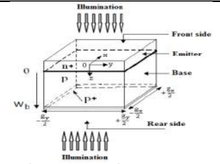 Figure 1.b: Polycristalline Silicon columnar grain model

In this study, we assume that:

- the contribution of the emitter is neglected. We take into account only the base contribution [6],
- the illumination is uniform. We then have a generation rate depending only with base depth *z* [12];
- the existing crystalline field within the base is neglected
- in the simulation, we have equality between the grain size along x and y axes, ie gx= gy=g(square cross section), and that the recombination velocity at grain boundaries is perpendicular to the junction and independent to the generation rate under AM 1.5 [6-9].

2.1. Excess Minority Carriers Density

Considering the emitter as a dead (non active) area, the excess minority carrier distribution distribution in the base, seen as a greater contribution to the photo-conversion, is derived from the continuity equation [6-14]:

$$D(Kl,\phi)\times\left[\frac{\partial^2\delta(x,y,z)}{\partial x^2}+\frac{\partial^2\delta(x,y,z)}{\partial y^2}+\frac{\partial^2\delta(x,y,z)}{\partial z^2}\right]-\frac{\delta(x,y,z)}{\tau}+G(z)=0 \quad (1)$$

$D(Kl,\phi)$ is the diffusion coefficient in the presence of irradiation. It is expressed as follows:

$$D(Kl,\phi)=\frac{L(Kl,\phi)^2}{\tau} \quad (2)$$

In this expression, G(z) represents the generation rate of minority charge carriers in the base [15] whose expression is given by the following equation:

$$G(z)=\sum_{i=1}^{3}a_i\times\exp(-b_i\times z) \quad (3)$$

The values ai and bi are the values tabulated from the modeling of the absorption spectrum of the photocell for AM 1.5 [9] [11] [19].

L depend on the irradiation energy Φ and the damage coefficient Kl through the following expression [19]-[21]:

$$L(Kl,\phi)=\sqrt{\frac{1}{\frac{1}{L_0^2}+Kl\times\phi}} \quad (4)$$

L_0 is the diffusion length without irradiation.

The solution of the equation can be written as follows [6] [9] [22]:

$$\delta(x,y,z)=\sum_k\sum_j Z_{k,j}(z)\times\cos(C_k\times x).\cos(C_j\times y) \quad (5)$$

k, j : are the indices for the x and y directions respectively.

Ck and Cj are obtained from the conditions at the grain boundaries $\pm\frac{g_x}{2}$ et $\pm\frac{g_y}{2}$ [6-9-11-23]:

$$\left[\frac{\partial\delta(x,y,z)}{\partial x}\right]_{x=\pm\frac{g_x}{2}}=\mp\frac{Sgb}{D(Kl,\phi)}\delta\left(\pm\frac{g_x}{2},y,z\right) \quad (6)$$

$$\left[\frac{\partial\delta(x,y,z)}{\partial y}\right]_{y=\pm\frac{g_y}{2}}=\mp\frac{Sgb}{D(Kl,\phi)}\delta\left(x\pm\frac{g_y}{2},z\right) \quad (7)$$

gx is the grain width, gy the grain length Sgb the recombination velocity at the grain boundaries.

From equations (6) and (7) we obtain two transcendental equations [30] which are:

$$\tan\left(C_k\times\frac{g_x}{2}\right)=\frac{Sgb}{2.C_k\times D(Kl,\phi)} \quad (8)$$

$$\tan\left(C_j\times\frac{g_y}{2}\right)=\frac{Sgb}{2.C_j\times D(Kl,\phi)} \quad (9)$$

By replacing δ(x, y, z) in the continuity equation and the fact that the cosine function is orthogonal, we obtain the following differential equation:

$$Z_{k,j}=A_{k,j}\times\cosh\left(\frac{z}{L_{k,j}}\right)+B_{k,j}\times\sinh\left(\frac{z}{L_{k,j}}\right)-\sum_{i=1}^{3}K_{i,j,k}\times\exp(-b_i\times z) \quad (10)$$

Or

$$K_{i,j,k}=\frac{L_{k,j}^2}{D_{k,j}\times\left[b_i^2\times L_{k,j}^2-1\right]}\times a_i \quad (11)$$

With :

$$L_{k,j}=\left[C_k^2+C_j^2+\frac{1}{L(Kl,\phi)^2}\right]^{-\frac{1}{2}} \quad (12)$$

And

$$D_{k,j}=D(Kl,\phi)\times\frac{\left[C_k\times g_x+\sin(C_k\times g_x)\right].\left[C_j\times g_y+\sin(C_j\times g_y)\right]}{16.\sin\left(C_k\times\frac{g_x}{2}\right).\sin\left(C_j\times\frac{g_y}{2}\right)}$$

(13)

The coefficients Ak,j and Bk,j are calculated from the following boundary conditions [2-6-10-15-27]:

- At the junction ($z = 0$) :

$$\left[\frac{\partial\delta(x,y,z)}{\partial z}\right]_{z=0} = \frac{Sf}{D(Kl,\phi)}\delta(x,y,0) \tag{14}$$

Sf is the junction recombination velocity, written as [2-6-10-15-27] Sf = Sf_0 + Sf_j with Sf_0 being the intrinsic junction recombination velocity related to the shunt resistance due to losses occurring across the junction and Sf_j is the imposed junction recombination velocity due external load. It defines the current flow that is the operating point of the cell. For each illumination mode, the intrinsic junction recombination velocity was calculated using the method described in

At the back side ($z = \omega b$):

$$\left[\frac{\partial\delta(x,y,z)}{\partial z}\right]_{z=0} = -\frac{Sb}{D(Kl,\phi)}\delta(x,y,\omega b) \tag{15}$$

Sb is the back surface recombination velocity. It quantifies the rate at which excess minority carriers are lost at the back surface of the cell [2-6-10-27]. The derivation of the photocurrent with respect to Sf, provides for each illumination mode the expression of Sb,

$$A_{k,j} = \sum_{i=1}^{3} K_{i,k,j} \times \frac{\frac{1}{L_{k,j}}.\left(\frac{Sf}{D(Kl,\phi)} - b_i\right) \times \exp(-b_i \times \omega b) + Y_{k,j}\left(\frac{Sf}{D(Kl,\phi)} + b_i\right)}{\frac{Sf \times Y_{k,j}}{D(Kl,\phi)} + \frac{X_{k,j}}{L_{k,j}}} \tag{16}$$

$$B_{k,j} = \sum_{i=1}^{3} K_{i,k,j} \times \frac{\frac{Sf}{D(Kl,\phi)}.\left(\frac{Sb}{D(Kl,\phi)} - b_i\right) \times \exp(-b_i \times \omega b) + X_{k,j}\left(\frac{Sf}{D(Kl,\phi)} + b_i\right)}{\frac{Sf \times Y_{k,j}}{D(Kl,\phi)} + \frac{X_{k,j}}{L_{k,j}}} \tag{17}$$

$$B_{k,j} = \sum_{i=1}^{3} K_{i,k,j} \times \frac{\frac{Sf}{D(Kl,\phi)}.\left(\frac{Sb}{D(Kl,\phi)} - b_i\right) \times \exp(-b_i \times \omega b) + X_{k,j}\left(\frac{Sf}{D(Kl,\phi)} + b_i\right)}{\frac{Sf \times Y_{k,j}}{D(Kl,\phi)} + \frac{X_{k,j}}{L_{k,j}}}$$

With:

$$X_{k,j} = \frac{1}{L_{k,j}} \times \sinh\left(\frac{\omega b}{L_{k,j}}\right) + \frac{Sb}{D(Kl,\phi)} \times \cosh\left(\frac{\omega b}{L_{k,j}}\right) \tag{18}$$

$$Y_{k,j} = \frac{1}{L_{k,j}} \times \cosh\left(\frac{\omega b}{L_{k,j}}\right) + \frac{Sb}{D(Kl,\phi)} \times \sinh\left(\frac{\omega b}{L_{k,j}}\right) \tag{19}$$

2.2. Photocurrent Density

The photocurrent density can be calculated by the following equation [6-9-12-28-29].

$$J_{ph} = \frac{q \times D(Kl,\phi)}{g_x \times g_y}.\int_{-\frac{g_x}{2}}^{+\frac{g_x}{2}}\int_{-\frac{g_y}{2}}^{+\frac{g_y}{2}}\left[\frac{\partial\delta(x,y,z)}{\partial z}\right]_{z=0} dx.dy \tag{20}$$

After calculation we get:

$$J_{ph}(Sf,Kl,\phi) = q \times \sum_{k=1}^{5}\sum_{j=1}^{5} R_{k,j} \times Sf.\sum_{i=1}^{3} K_{i,k,j}.\frac{\frac{Sb - D(Kl,\phi) \times b_i}{D(Kl,\phi) \times Y_{k,j}} - \frac{X_{k,j}}{Y_{k,j}} + b_i \times L_{k,j}}{\frac{X_{k,j}}{Y_{k,j}} + \frac{Sf \times L_{k,j}}{D(Kl,\phi)}} \tag{21}$$

With,

$$R_{k,j} = \frac{4.\sin\left(C_k \times \frac{g_x}{2}\right) \times \sin\left(C_k \times \frac{g_y}{2}\right)}{g_x \times g_y \times C_k \times C_j} \tag{22}$$

q is the charge of the electron.

2.3. Photo Voltage

Using the Boltzmann's relation, the photo voltage Vph can be expressed as [6] [9] [28]:

$$V_{ph} = V_T.\ln\left\{1 + \frac{N_b}{n_i^2}.\int_{-\frac{g_x}{2}}^{+\frac{g_x}{2}}\int_{-\frac{g_y}{2}}^{+\frac{g_y}{2}}\delta(x,y,z).dx.dy\right\} \tag{23}$$

When the photocell is illuminated simultaneously by the front and rear sides, the photovoltage is given by the following expression:

$$V_{ph} = V_T.\ln\left\{1 + \frac{N_b}{n_i^2}.\sum_{k=0}^{4}\sum_{j=0}^{4} R_{k,j}.\sum_{i=1}^{3} K_{i,k,j}.\frac{\frac{Sb - D(Kl,\phi).b_i}{D(Kl,\phi).Y_{k,j}}.\exp(-b_i \times H) - \frac{X_{k,j}}{Y_{k,j}} + b_i \times L_{k,j}}{\frac{X_{k,j}}{Y_{k,j}} + \frac{Sf \times L_{k,j}}{D(Kl,\phi)}}\right\} \tag{24}$$

$V_T = \frac{k \times T}{q}$ is the thermal voltage, k the Boltzmann constant, Nb the base doping rate and ni the intrinsic carrier concentration.

3. RESULTS AND DISCUSSIONS

3.1. Effect of the irradiation energy on the current density

The Figure 2 plots the current density as a function of the recombination velocity at the junction, of a front-illuminated photocell. We considered increasing irradiation energies Φ, grain sizes, recombination velocities at the grain boundaries and damage coefficients are fixed.

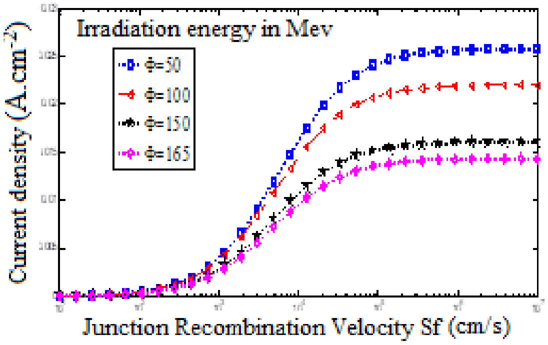

Figure 2: Current density as a function of the recombination rate at the Sfj junction for a grain size g=0.0005 cm and different irradiation energies Sgb=4,5*10^{6}cm/s; Kl=10,5 cm^{-2}/MeV; ωb=0.03 cm and AM 1.5

The current density increases with the recombination rate at the junction. The evolution of the current density presents two remarkable levels:

- one in an open-circuit situation where the current density is almost zero,
- the other in short-circuit situation where the current density is maximum.

Between the two situations mentioned above, the operating point of the solar cell varies. The increase of the irradiation energy leads to a decrease of the amplitude of the current density. The explanation that can be drawn from this is that the irradiation energy reduces the mobility of the carriers at the junction. But also, it blocks the carriers, thus, the concentration of the carriers increases, hence a decrease of the current density;

3.2. Effect of the damage coefficient Kl on the current density

We plot in the following Figure 3 the current density versus the recombination rate at the junction for different damage coefficients. For this, we fix the grain size, the recombination velocity at the grain boundary and the irradiation energy.

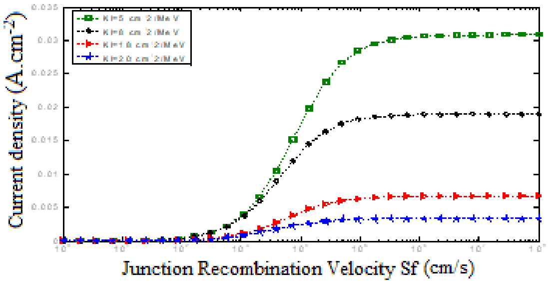

Figure 3: Current density as a function of recombination rate at the Sfj junction for grain size g=0.0005 cm and different damage coefficients, Sgb=4,5*10^{6}cm/s; Φ=150 MeV; ωb=0.03 cm and AM 1.5

Figure 3 shows that the current density decreases when the damage coefficient goes from low to high values. The explanation is that the increase of the damage coefficient reflects an increase in the probability of creation of defects by irradiation, thus of more important degradation of the solar cell, i.e., more important leakages.

3.3. Effect of the irradiation energy on the photovoltage

The Figure 4 represents the photovoltage as a function of the recombination rate at the junction of the same solar cell illuminated by four increasing irradiation energies.

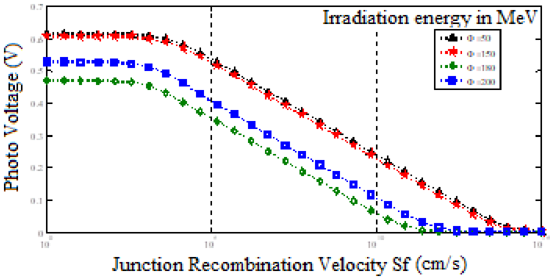

Figure 4: Photovoltage versus recombination rate at the Sfj junction for a grain size g= 0.0005cm and different irradiation energies,

Sgb=4,5*10^{6}cm/s; Kl=10,5 cm^{-2}/MeV ; ωb=0.03 cm and AM 1.5

The curves Figure 4 of photovoltage versus Sfj for different values of the irradiation energy show levels for low recombination rates at the junction, in this area the photovoltage is maximum. It corresponds to the open circuit. There is storage of carriers at the junction. However, when the speed of recombination exceeds a certain value, the photovoltage which coincides with the limit of the zero current density, decreases very quickly to cancel at high speeds of recombination at the junction Sfj: this is the operation of the photocell in short-circuit which is a point of operation where the photocell delivers a maximum current and a zero voltage

We also note a decrease in photo tension with the energy of irradiation; if we vary the energy of irradiation, we observe that the photo tension decreases when the energy of irradiation increases; this decrease being more accentuated for energies of irradiation too high. Indeed, if the irradiation energy increases, it means that the material becomes more sensitive to degradation caused by possible particles and therefore the photo tension will be more degraded as the irradiation energy increases.

3.4. Effect of the irradiation energy on the photovoltage

We plot in the following figure 5 the photovoltage versus the recombination rate at the junction for different damage coefficients. For this purpose, we fix the grain sizes, the recombination rate at the grain boundaries and the irradiation energy.

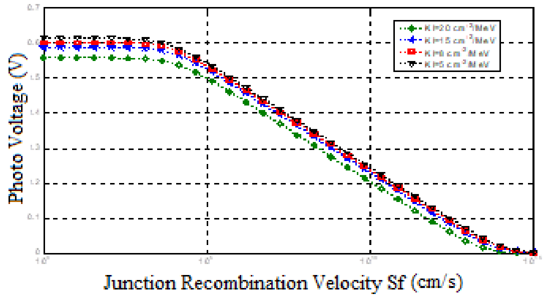

Figure 5: Photovoltage as a function of recombination rate at the Sfj junction for grain size g= 0.0005 cm and different damage coefficients, Sgb=4.5*10^{6}cm/s; Φ=150 MeV, ωb=0.03 cm and AM 1.5

Let us note on Figure 5 that this decrease of the photovoltage is especially marked when the photocell works in the vicinity of the open circuit; indeed, in the vicinity of the open circuit, the carriers are accumulated in the vicinity of the junction thus increasing the probability of interaction with the irradiating particles and thus the degradations

3.5. Effect of the irradiation energy Φ on the I-V characteristic of the photocell

The current-voltage characteristic giving the profile of the current density as a function of photovoltage when Sfj varies and for different values of the irradiation energy when the grain size, the recombination rate at the grain boundaries and the damage coefficient are fixed.

Figure 6 represents the evolution of the current density as a function of photovoltage by varying the irradiation energy.

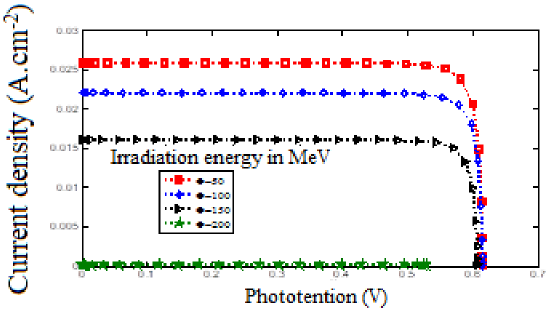

Figure 6: Current density as a function of photo voltage for grain size g=0.0005 cm and different irradiation energies, Sgb=4,5*10^6cm/s; Kl=10,5 cm^{-2}/MeV ; ωb=0.03 cm and AM 1.5

We observe here that the current-voltage characteristic decreases with the irradiation energy; indeed, when the irradiation energy increases, the degradations caused are more important within the material which leads to a decrease of the current density and the photovoltage.

3.6. Effect of the damage coefficient Kl on the I-V characteristic of the photocell

We plot in Figure 7 the current-voltage characteristic of the bifacial photocell illuminated by its front side for different values of damage coefficients.

This Figure 7 shows the effect of the damage coefficient on the open circuit and the short circuit.

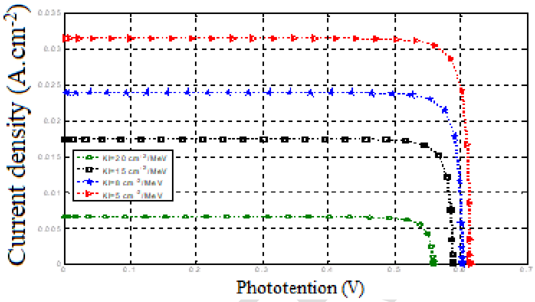

Figure 7: Current density as a function of photo voltage for grain size g=0.0005 cm and different damage coefficient values, Sgb=4,5*10^6cm/s; Φ=150 MeV ; ωb=0.03 cm and AM 1.5

We can always note on the Figure 7 that the current-voltage characteristic decreases with the damage coefficient; this decrease being more accentuated for the high damage coefficients. Indeed, if the damage coefficient increases, it means that the material becomes more sensitive to degradation caused by particles and therefore the current density and photovoltage will be more degraded as the damage coefficient increases.

4. CONCLUSION

In this paper we have made a three-dimensional study of a polycrystalline silicon photocell in the static regime under irradiation and multispectral illumination. This study has shown us that the minority charge carrier density, the current density and the photovoltage of the photocell believe with the irradiation (ϕ, Kl). In summary the irradiation energy (Φ) and the damage coefficient (Kl) reduce the performance of the photocell.

REFERENCES

1. M. L. Samb, S. Sarr, S. Mbodji, S. Gueye, M. Dieng and G. Sissoko, (2009), Study in 3-D modeling of a silicon photocell in static regime under multispectral illumination multispectral: determination of the electrical parameters, J. Sci. Vol. 9, N°. 4, pp. 36 –50; http ://www.cadjds.org.
2. S. Mbodji, A. S. Maiga, M. Dieng, A.Wereme and G. Sissoko, (2010), Renoval charge technic applied to a bifacial solar cell under constant magnetic field Global Journal of Pure and Applied Sciences Vol. 16, N0. 4, pp. 469- 477. http://www.globaljournalseries.com
3. S. Madougou, Nzonzolo, S. Mbodji,F. Barro and G. Sissoko, (2004) , Bifacial silicon solar cell space charge region width determination by a study in modelling: effect of the magnetic field, J. Sci. Vol. 4, N° 3, pp. 116-123; http://www.cadjds.org
4. F. I. Barro, S. Mbodji, M. Ndiaye, E. Ba and G. Sissoko, (2008), Influence of grains size and grains boundaries recombination on the space-charge layer thickness z of emitter-base junction's n+-p-p+ solar cell Proceedings of the 23rd European Photovoltaic Solar

Energy Conference, pp. 604-607. DOI : 10.4229/23rdEUPVSEC 2008-1CV.2.63 ;http://www.eupvsec proceedings.com

5. M. L. Samb, M. Dieng, S. Mbodji, B. Mbow, N. Thiam, F.I. Barro and G. Sissoko.(2009),Recombinationparameters measurement of silicon solar cell under constant white bias light. Proceedings of the 24th European Photovoltaic Solar Energy Conference, pp. 469-472,DOI: 10.4229/24thEUPVSEC2009-1CV.4.15; http://www.eupvsec-proceedings.com
6. H. L. Diallo, A. Wereme, A. S. Maïga and G. Sissoko, (2008), New approach of both junction and back surface recombination velocities in a 3D modeling study of a polycrystalline silicon solar cell. Eur. Phys. J. Appl. Phys., 42, pp. 203–211.
7. Dieng, M. L. Sow, S. Mbodji, M. L. Samb, M. Ndiaye, M. Thiame, F.I. Barro and G. Sissoko, (2009), 3D Study of a Polycrystalline Silicon Solar Cell: Influence of Applied Magnetic Field on the Electrical Parameters. Proceedings of the 24th EuropeanPhotovoltaic Solar Energy Conference, pp .473-476,DOI: 10.4229/24thEUPVSEC2009-1CV.4.16; http://www.eupvsec-proceedings.com
8. B. Zouma, A. S. Maiga, M. Dieng, F. Zougmore, G. Sissoko, (2009), 3D Approach of spectral response for a bifacial silicon solar cell under a constant magnetic field Global Journal of Pure and Applied Sciences, Vol.15, N°1, 2009, pp. 117-124; http://www.globaljournalseries.com
9. J. Dugas, (1994), 3 D Modelling of a Reverse Cell Made with improved Multycrystalline Silicon Wafers, Solar Energy Materials and Solar Cells, Vol.32, No 1, pp.71-88.
10. S.Mbodji, M.Dieng, B.Mbow, F.I.Barro and G.Sissoko; (2010) Three dimensional simulated modelling of diffusion capacitance of polycrystalline bifacial silicon solar cell. Journal of Applied Sciences and Technology (JAST) Vol. 15, Nos.1&2, pp. 109-114;
11. S. R. Dhariwal, (1988), Photocurrent and photovoltage from polycrystalline p-n junction Solar Cells, Vol. 25, pp. 223-233, (1988).
12. H. El Ghitani And S. Martinuzzi, (1989), Influence of dislocations on electrical properties of large grained polycrystalline silicon cells. I. Model. J. Appl. Phys., Vol. 66, N°4, pp. 1717-1722.
13. Muzeyyen Saritas and Harry D. Mckell, (1988), Comparison of Minority-Carrier Diffusion Length Measurements in Silicon by the Photoconductive Decay and Surface Photovoltage Methods, J. Appl. Phys. 63 (9), pp. 4561-4567. http://www.inasp.info/ajol
14. Mbodji, S., Mbow, B., Barro, F.I. and Sissoko, G., (2011), A 3D Model for Thickness and Diffusion Capacitance of Emitter-Base Junction Determination in a Bifacial Polycrystalline Solar Cell under Real Operating Condition. Turkish Journal of Physics, Vol. 15, pp. 281-291.
15. Jose Furlan and Slavko Amon, (1985), Approximation of the carrier generation rate in illuminated silicon, Solid State Electr, Vol.28, N0 .12, pp.1241-1243.
16. R. J. Walters and G. P. Summers, (2002), Space Radiation Effects in Advanced Solar Cell Materials and Devices Mat. Res. Soc. Symp. Proc. Vol. 692, pp. 569-580.

17. M.A. Ould El Moujtaba, M. Ndiaye, A.Diao, M.Thiame, I.F. Barro and G. Sissoko. (2002), Theoretical Study of the Influence of Irradiation on a Silicon Solar Cell under Multispectral Illumination. Research Journal of Applied Sciences, Engineering and Technology, 4(23): pp. 5068-5073.
18. R. K. Ahrenkiel, D. J. Dunlavy, H. C. Hamaker, R. T. Green, C. R. Lewis, R. E. Hayes, H. Fardi, (1986), Time-of-flight studies of minority-carrier diffusion in AlxGa1-xAs homojunctions , J. Appl. Phys. 49(12) 1986.
19. J. Oualid and C. M. Singal, (1984), Influence of illumination on the grain boundaries recombination velocity in silicon J. Appl. Phys. 55(4), pp. 1195-1205.
20. Alfred Dieng, Ndeye Thiam, Mamadou Lamine Samb, Amadou Seïdou Maïga, Fabé Idrissa Barro, Grégoire Sissoko, (2009), 3d study of a polycrystalline silicon photocell influence of grain size and recombination rate at the grain boundaries on the electrical grain boundaries on the electrical parameters, Journal of Science, Vol. 9, N0 1, pp. 51-63. http:// www. ucadjds. org.
21. H. Shimizu, K. Kinamery, N. Honma and Chusuke Munakata Japanese, (1987), Determination of Surface Charge and Interface Trap Densities in Naturally Oxidize n-type Si Wafers Using Surface Photovoltages, journal of applied physics, Vol.26, No .12, December, pp. 2033-2036.
22. M.C Halder and T.R.Williams, (1983), Grain boundary effects in polycrystalline Silicon SolarCells I. Solution of the three-Dimensional diffusion equation by the Green's function method, Solar Cells, Vol. 8, No 3, pp. 201-223.
23. Nzonzolo, Lilonga-Boyenga, D., Mabika, C.N. and Sissoko, G., (2016), Two- Dimensional Finite Element Method Analysis Effect of the Recombination Velocity at the Grain Boundaries on the Characteristics of a Polycrystalline Silicon Solar Cell. Circuits and Systems, 7, pp. 4186-4200. http://dx.doi.org/10.4236/cs.2016.713344.
24. G. Sissoko, E. Nanéma, A. Corréa, P. M. Biteye, M. Adj, A. L. Ndiaye, (1998), Silicon Solar cell recombination parameters determination using the characteristic. Renewable Energy, Vol-3, pp.1848-185.1 Elsevier Science Ltd, 0960-1481/98/#.
25. G. Sissoko, C. Museruka, A. Correa, I. Gaye, A. L. Ndiaye, (1996), Light spectral effect on recombination parameters of silicon solar cell. In Proceedings of the World Renewable Energy Congress, Denver, USA, pp.1487-1490.
26. Y. L. B. Bocande, A. Correa, I. Gaye, M. L. Sow and G. Sissoko, (1994), Bulk and surfaces parameters determination in high efficiency Si solar cells. Renewable Energy, Vol 5, part III, pp. 1698-1700, Pergamon, 0960-1481.
27. M. Ndiaye, A. Diao, M. Thiame, M. M. Dione, H. LY. Diallo, M. L. Samb, I. Ly, Gassama, S. mbodji, F. I. Barro and G. Sissoko, (2010) 3D Approach for a Modelling Study of the Diffusion Capacitance's Efficiency of the Solar Cell; Proceedings of 25 th European Photovoltaic Solar Energy Conference and Exhibition, Valencia, Spain, pp. 484-487.
28. M. M. Dione, I. Ly, A. Diao, S. Gueye, A. Gueye, M. Thiame, G. Sissoko, (2013), Determination of the impact of the grain size and

the recombination velocity at grain boundary on the values of the electrical parameters of a bifacial polycristallin silicon solar cell, IRACST – Engineering Science and Technology: International Journal, Vol.3, N0. 1, pp. 66-73.

29. Adel Ben Arab, (1995), Photovoltaic properties and high efficiency of preferentially doped polysilicon solar cells Solid-State Electronics, Vol. 38, N°. 8, pp. 1441-1447.

30. M. M. Deme, S. Mbodji, S. Ndoye, A. Thiam, A. Dieng and G. S; (2010), Influence of illumination incidence angle, grain size and grain boundary recombination Velocity on the facial solar cell diffusion capacitance; Revue des Energies Renouvelables Vol. 13, N°1, pp. 109-121.